NeuroImage: Clinical 27 (2020) 102300

Contents lists available at ScienceDirect

NeuroImage: Clinical

journal homepage: www.elsevier.com/locate/ynicl

"Switchboard" malfunction in motor neuron diseases: Selective pathology of thalamic nuclei in amyotrophic lateral sclerosis and primary lateral sclerosis

Rangariroyashe H. Chipika[a], Eoin Finegan[a], Stacey Li Hi Shing[a], Mary C. McKenna[a], Foteini Christidi[a,b], Kai Ming Chang[a,c], Mark A. Doherty[d], Jennifer C. Hengeveld[d], Alice Vajda[d], Niall Pender[e], Siobhan Hutchinson[f], Colette Donaghy[g], Russell L. McLaughlin[d], Orla Hardiman[a], Peter Bede[a,*]

[a] Computational Neuroimaging Group, Biomedical Sciences Institute, Trinity College Dublin, Ireland
[b] Department of Neurology, Aeginition Hospital, University of Athens, Greece
[c] Electronics and Computer Science, University of Southampton, United Kingdom
[d] Complex Trait Genomics Laboratory, Smurfit Institute of Genetics, Trinity College Dublin, Ireland
[e] Department of Psychology, Beaumont Hospital Dublin, Ireland
[f] Department of Neurology, St James's Hospital, Dublin, Ireland
[g] Department of Neurology, Western Health & Social Care Trust, Belfast, United Kingdom

ARTICLE INFO

Keywords:
Motor neuron disease
Amyotrophic lateral sclerosis
Primary lateral sclerosis
Thalamus
Thalamic nuclei
Neuroimaging

ABSTRACT

The thalamus is a key cerebral hub relaying a multitude of corticoefferent and corticoafferent connections and mediating distinct extrapyramidal, sensory, cognitive and behavioural functions. While the thalamus consists of dozens of anatomically well-defined nuclei with distinctive physiological roles, existing imaging studies in motor neuron diseases typically evaluate the thalamus as a single structure. Based on the unique cortical signatures observed in ALS and PLS, we hypothesised that similarly focal thalamic involvement may be observed if the nuclei are individually evaluated. A prospective imaging study was undertaken with 100 patients with ALS, 33 patients with PLS and 117 healthy controls to characterise the integrity of thalamic nuclei. ALS patients were further stratified for the presence of GGGGCC hexanucleotide repeat expansions in *C9orf72*. The thalamus was segmented into individual nuclei to examine their volumetric profile. Additionally, thalamic shape deformations were evaluated by vertex analyses and focal density alterations were examined by region-of-interest morphometry. Our data indicate that *C9orf72* negative ALS patients and PLS patients exhibit ventral lateral and ventral anterior involvement, consistent with the 'motor' thalamus. Degeneration of the sensory nuclei was also detected in *C9orf72* negative ALS and PLS. Both ALS groups and the PLS cohort showed focal changes in the mediodorsal-paratenial-reuniens nuclei, which mediate memory and executive functions. PLS patients exhibited distinctive thalamic changes with marked pulvinar and lateral geniculate atrophy compared to both controls and *C9orf72* negative ALS. The considerable ventral lateral and ventral anterior pathology detected in both ALS and PLS support the emerging literature of extrapyramidal dysfunction in MND. The involvement of sensory nuclei is consistent with sporadic reports of sensory impairment in MND. The unique thalamic signature of PLS is in line with the distinctive clinical features of the phenotype. Our data confirm phenotype-specific patterns of thalamus involvement in motor neuron diseases with the preferential involvement of nuclei mediating motor and cognitive functions. Given the selective involvement of thalamic nuclei in ALS and PLS, future biomarker and natural history studies in MND should evaluate individual thalamic regions instead overall thalamic changes.

1. Introduction

While amyotrophic lateral sclerosis (ALS) is a clinically and genetically heterogeneous neurodegenerative condition, patients with ALS have a relatively stereotyped disease trajectory dominated by relentlessly progressive motor disability and ultimately respiratory compromise. The core neuroimaging signature of ALS includes motor cortex, brainstem, corticospinal tract, and spinal cord degeneration.

* Corresponding author at: Room 5.43, Computational Neuroimaging Group, Trinity Biomedical Sciences Institute, Trinity College Dublin, Pearse Street, Dublin 2, Ireland.
E-mail address: bedep@tcd.ie (P. Bede).

https://doi.org/10.1016/j.nicl.2020.102300
Received 12 February 2020; Received in revised form 22 May 2020; Accepted 23 May 2020
Available online 30 May 2020

Subcortical grey matter degeneration has also been observed both post mortem and in vivo (Westeneng et al., 2015). Thalamus pathology in ALS has been evaluated by dedicated structural, metabolic, and functional imaging studies (Machts et al., 2015; Cistaro et al., 2014; Sharma et al., 2011; Lule et al., 2010; Tu et al., 2018). The thalamus however is typically evaluated as a single structure in ALS. Overall thalamic atrophy has been identified by both neuroimaging (Machts et al., 2015; Menke et al., 2014; Chang et al., 2005) and post mortem histopathology studies in ALS (Neumann et al., 2006), but the involvement of specific nuclei has not been comprehensively characterised to date. The thalamus comprises over 60 cytoarchitectonically distinct nuclei with unique cortical connectivity patterns (Behrens et al., 2003), physiological functions, (Bosch-Bouju et al., 2013) embryonic origin, (Blackshaw et al., 2010) and vascular supply (Schmahmann, 2003). The risk of evaluating the entire thalamus as a whole is averaging pathological change across affected and unaffected regions. Several radiological approaches exist to segment the thalamus; it may be parcellated based on cortical connectivity patterns (Behrens et al., 2003; Johansen-Berg et al., 2005; Zhang et al., 2017) or anatomically, based on the histological data (Iglesias et al., 2018). The few existing thalamus studies in ALS segmented the thalamus based on cortical projection patterns (Tu et al., 2018; Bede et al., 2018) and not anatomically, which would allow the systematic assessment of specific nuclei.

Given the strikingly focal cortical grey matter signatures observed in both ALS (Lule et al., 2010) and PLS (Clark et al., 2018) we hypothesised that similarly selective thalamic involvement may be detected if thalamic nuclei are appraised individually. Irrespective of the underlying genotype, co-existence of cognitive deficits, familial or sporadic presentation, limb weakness and bulbar impairment are pathognomonic clinical features of ALS (Kiernan et al., 2011) which can be linked to motor cortex and spinal cord degeneration on imaging (Querin et al., 2018). Based on clinical and radiological observations, it is increasingly clear that extra-pyramidal degeneration also contributes to motor disability in ALS (Pradat et al., 2009; Feron et al., 2018). Connectivity-based thalamic segmentation in ALS reveals focal degeneration in thalamic regions projecting to motor areas (Bede et al., 2018) and frontotemporal regions (Tu et al., 2018). Accordingly, we hypothesised that thalamic pathology in ALS preferentially involves nuclei mediating motor function such as the ventral anterior and ventral lateral nuclei.

While GGGGCC hexanucleotide expansions in *C9orf72* in ALS have been previously linked to orbitofrontal (Floeter et al., 2016); opercular (Bede et al., 2013a), cingulate (Cistaro et al., 2014) and temporal lobe alterations (Floeter et al., 2018), widespread extra-motor (Westeneng et al., 2016) and subcortical grey matter changes (Bede et al., 2013b) are also readily observed in *C9orf72* negative sporadic ALS patients. The *C9orf72* genotype has also been linked to thalamus pathology in ALS (Cistaro et al., 2014; Bede et al., 2013b), but that thalamic signature of C9orf72-associated ALS has not been characterised at a nuclear level. A recent large FTD study (Bocchetta et al., 2020) identified that *C9orf72* hexanucleotide repeat carriers exhibit preferential pulvinar atrophy, which is thought to be unique to the genotype. Based on the available FTD literature (Bocchetta et al., 2020; Bocchetta et al., 2018; Mahoney et al., 2012; Irwin et al., 2013), one of the objectives of this study is to examine if *C9orf72* mutation carriers in ALS exhibit distinctive patterns of thalamic involvement different from sporadic ALS patients. As GGGGCC hexanucleotide repeat expansions in ALS are associated with neuropsychological deficits (Byrne et al., 2012), we hypothesised that *C9orf72* positive ALS patients may exhibit preferential degeneration in thalamic nuclei mediating cognitive functions.

In contrast to ALS, there is a striking paucity of both imaging and post mortem studies in PLS (Clark et al., 2018). PLS is associated with longer survival than ALS (Gordon et al., 2006) and the clinical picture is dominated by upper motor neuron dysfunction (Floeter and Mills, 2009). Extra-motor (de Vries et al., 2019) and extra-pyramidal (Le Forestier and Meininger, 2009) manifestations have been sporadically reported in PLS, but thalamic involvement has not been systematically characterised to date in vivo. As clinical heterogeneity is less marked in PLS than ALS, we hypothesised that focal changes will be captured in the ventral anterior and ventral lateral nuclei.

While the clinical symptoms of ALS and PLS are dominated by limb weakness, bulbar impairment and respiratory weakness, sensory deficits have also been reported, captured by electrophysiology studies and sensory tract involvement detected on spinal imaging (Iglesias et al., 2015; Sangari et al., 2018). Patients with ALS often report paraesthesiae, but frank nociceptive, thermoceptive or proprioceptive deficits are seldom detected on clinical assessment (Tao et al., 2018). The anatomical segmentation of the thalamus into specific nuclei permits the targeted assessment of ventral posterolateral nuclei which mediate somatosensory information from the contralateral face and the ventral medial nuclei conveying somatosensory information from the contralateral trunk and limbs.

Building on accruing evidence of overall thalamic involvement in ALS, the main objective of this study was the characterisation of regional thalamic pathology in sporadic, *C9orf72* negative ALS at a nuclear level. An additional objective was to evaluate if PLS and *C9orf72* positive ALS patients have distinctive thalamic signatures. Based on the review of the literature, we hypothesised, that the 'global' thalamus pathology reported by previous imaging studies in ALS is driven by focal changes in susceptible nuclei.

2. Methods

2.1. Ethics statement

All aspects of this study, including recruitment, data management, consent forms and information leaflets were approved by the institutional ethics committee (Beaumont Hospital, Dublin, Ireland), in accordance with the 1964 Helsinki declaration and its later amendments. Study participants provided informed consent prior to inclusion.

2.2. Participants

Patients were recruited between September 2017 and September 2020. Hundred patients with ALS, 33 patients with PLS and 117 healthy controls were included in this study. PLS patients were diagnosed based on the Gordon criteria (Gordon et al., 2006) Participating ALS patients had 'probable' or 'definite' ALS according to the El Escorial criteria (Brooks et al., 2000). Exclusion criteria included a known history of traumatic brain injury, cerebrovascular events, neuroinflammatory conditions, neoplastic conditions, and inability to undergo MRI scanning due to metallic devices such as baclofen pumps or pacemakers. Known claustrophobia or orthopnoea were other exclusion criteria. The demographic and clinical profile of each patient was carefully recorded; motor disability was assessed by the revised ALS functional rating scale (ALSFRS-r) (Cedarbaum et al., 1999), the Edinburgh Cognitive ALS Screen (ECAS) (Abrahams et al., 2014) was administered for cognitive assessment using population-based normative values (Pinto-Grau et al., 2017) and the diagnosis of co-morbid FTD was established based on the revised Strong criteria (Strong et al., 2017). The healthy controls of the study were unrelated to the participating patients and had no known neurological or psychiatric conditions, previous head injuries or a family history of neurodegenerative conditions.

2.3. Neuroimaging methods

T_1-weighted images were acquired with a 3D Inversion Recovery prepared Spoiled Gradient Recalled echo (IR-SPGR) pulse sequence on a 3 Tesla Philips Achieva system using an 8-channel receive-only head coil. The following pulse sequence parameters were used; field-of-view (FOV): 256 × 256 × 160 mm, spatial resolution: 1 mm^3, TR/TE = 8.5/3.9 ms, TI = 1060 ms, flip angle = 8°, SENSE factor = 1.5, acquisition

time: 7 min 30 s.

2.4. TIV volumes

Total intracranial volume (TIV) was estimated for each study participant to be used as a covariate in comparative statistical models. TIV was calculated by adding grey matter, white matter and CSF volume estimates. Registration and tissue type segmentation was carried out in FMRIB's FSL environment. Following skull-stripping (Smith, 2002) and individual quality verification, each subject image was linearly aligned to MNI152 standard space using FMRIB's Linear Image Registration Tool (FLIRT) (Jenkinson et al., 2002). Tissue-type segmentation was performed using FMRIB's Automated Segmentation Tool (FAST) (Zhang et al., 2001) which accounts for spatial intensity variations. The inverse of the determinant of the affine registration matrix was calculated and multiplied by the size of the template for tissue-type volume estimation.

2.5. Thalamic segmentation

A Bayesian inference was used to segment the thalamus into 25 subregions as described by Iglesias at al. using a probabilistic atlas developed based on histological data in the FreeSurfer analysis suite (Iglesias et al., 2018) (Fig. 1). The thalamus was parcellated into the following nuclei in each hemisphere: antero-ventral (AV), latero-dorsal (LD), lateral posterior (LP), ventral anterior (VA), ventral anterior magnocellular (VA mc), ventral lateral anterior (VLa), ventral lateral posterior (VLp), ventral posterolateral (VPL), ventromedial (VM), central medial (CeM), central lateral (CL), paracentral (Pc), centromedian (CM), parafascicular (Pf), paratenial (Pt), reuniens/medial ventral (MV-re), mediodorsal medial magnocellular (MDm), mediodorsal lateral parvocellular (MDl), lateral geniculate (LGN), medial geniculate (MGN), limitans/suprageniculate (L-SG), pulvinar anterior (PuA), pulvinar medial (PuM), pulvinar lateral (PuL), and pulvinar inferior (PuI). The raw volume estimates of the above nuclei were averaged between left and right and merged into the following 10 core group of nuclei defined based on their distinctive physiological function: "Anteroventral", "Lateral geniculate", "Medial geniculate", "Pulvinar-limitans" (PuA, PuM, PuL, PuI, L-SG), "Laterodorsal", "Lateroposterior", "Mediodorsal-paratenial-reuniens" (MDm, MDl, MV-re, Pt), "Motor hub" (VA, VAmc, VLa, VLp), "Sensory hub" (VPL, VM), "Intralaminar" (CeM, CL, Pc, CM, Pf). "Total thalamic volume" was defined as the mean of the left and right thalamus volume estimates.

2.6. Vertex analyses

Surface projected patterns of atrophy were evaluated using vertex analyses. As described previously (Machts et al., 2015), FMRIB's subcortical segmentation and registration tool FIRST (Patenaude et al., 2011) was utilised to characterise focal thalamic shape deformations. Vertex locations of each participant were projected on the surface of an average thalamic shape template as scalar values, positive value being outside the surface and negative values inside. The average thalamic shape was generated from all participants. Permutation based non-parametric inference was implemented for group comparisons using FMRIB's 'RANDOMISE' module (Winkler et al., 2014). The design matrices included demeaned age, gender, education, total intracranial volumes and education as covariates (Winkler et al., 2014).

2.7. Region of interest morphometry

In order to characterise focal pathology beyond shape deformations and volume reductions in the thalamus, region-of-interest morphometry was performed to explore focal density alterations. FMRIB's software library (FSL) was used for skull removal and tissue-type segmentation. Affine registration was used to align grey-matter partial volume images to the MNI152 standard space. A study-specific grey matter template was then created to which the grey matter images of each subject were non-linearly coregistered. The study specific template was generated by the same number of randomly selected subjects from each study group i.e. 12 C9 + ALS patients, 12 C9- ALS patients, 12 healthy controls and 12 PLS patients to ensure that the template is representative of each study group. A voxelwise generalized linear model and permutation-based non-parametric inference were utilised to evaluate density alterations in a bilateral thalamus mask accounting for age, gender, TIV and education (Winkler et al., 2014; Nichols and Holmes, 2002). The labels of the Harvard-Oxford probabilistic structural atlas (Desikan et al., 2006) was used to generate the bilateral thalamus mask.

2.8. Genetics

All ALS and PLS patients were tested for *C9orf72* repeat expansions and tested for a panel of mutations implicated in ALS and PLS. DNA samples were tested for pathogenic GGGGCC hexanucleotide repeat expansions by repeat-primed PCR using the Applied Biosystems (Foster City, CA, USA) 3130xl Genetic Analyser and visualised using GeneMapper version 4.0. More than 30 hexanucleotide repeats were considered pathological. All patients were also tested for an extensive panel of ALS and PLS associated mutations including *SOD1, ALS2, SETX, SPG11, FUS, VAPB, ANG, TARDBP,* Fig. 4*, OPTN, ATXN2, VCP, UBQLN2, SIGMAR1, CHMP2B, PFN1, ERBB4, HNRNPA1, MATR3, CHCHD10, UNC13A, DAO, DCTN1, NEFH, PRPH, SQSTM1, TAF15, SPAST, ELP3, LMNB1, SARM1, C21orf2, NEK1, FUS, CHMP2B, GRN, MAPT, PSEN1, PSEN2, TBK1*. Sixty-seven ALS patients and all 33 PLS patients underwent whole genome sequencing (Project MinE, 2018) and the remaining 33 ALS patients underwent target next –generation targeted sequencing (Kenna et al., 2013). In addition to *C9orf72* testing and genetic screening for established ALS-causing mutations, PLS patients were also screened for a panel of 70 genes linked to HSP (Finegan et al., 2019a; Klebe et al., 2015). ALS patients were stratified based on their *C9orf72* status. Inclusion criteria for the *C9orf72* positive ALS group were patients who carried the GGGGCC repeat expansions but tested negative for other established mutations associated with ALS. Inclusion criteria for the *C9orf72* negative ALS group were patients who tested negative for *C9orf72* hexanucleotide repeat expansions as well as other established mutations associated with ALS. All PLS patients included in this study tested negative for the *C9orf72* repeat expansions as well as mutations associated with ALS and HSP.

2.9. Statistical analysis

The statistical interpretation of demographic and clinical data was conducted using IBM Statistical Product and Service Solutions (SPSS) version 25. Group differences in age, education and ALSFRS-r were examined using multivariate analysis of variance (MANOVA). Differences in gender, handedness, disease onset, and the proportion of patients with cognitive impairment were assessed with Chi-square tests. Intergroup differences in thalamic volumes were also evaluated in SPSS. Assumptions of normality were examined using the Kolmogorov-Smirnov test separately for each group. Since all variables followed a normal distribution, parametric statistics were used. Intergroup differences in thalamic volumes were examined using multivariate analysis of covariance with total intracranial volume (TIV), age, gender and education as covariates. If a significant main effect of group membership was identified ($p < 0.05$) for specific thalamic nuclei, post-hoc group comparisons were performed. False discovery rate (FDR-Benjamini Hochberg) corrections were used to account for multiple comparisons. The association between symptom duration and thalamic volumes was further examined in ALS and PLS patients with partial correlation, using age, gender, education and TIV as covariates. Correlations between motor disability (ALSFRS-r) and the volume of motor nuclei were also explored in PLS and ALS patients.

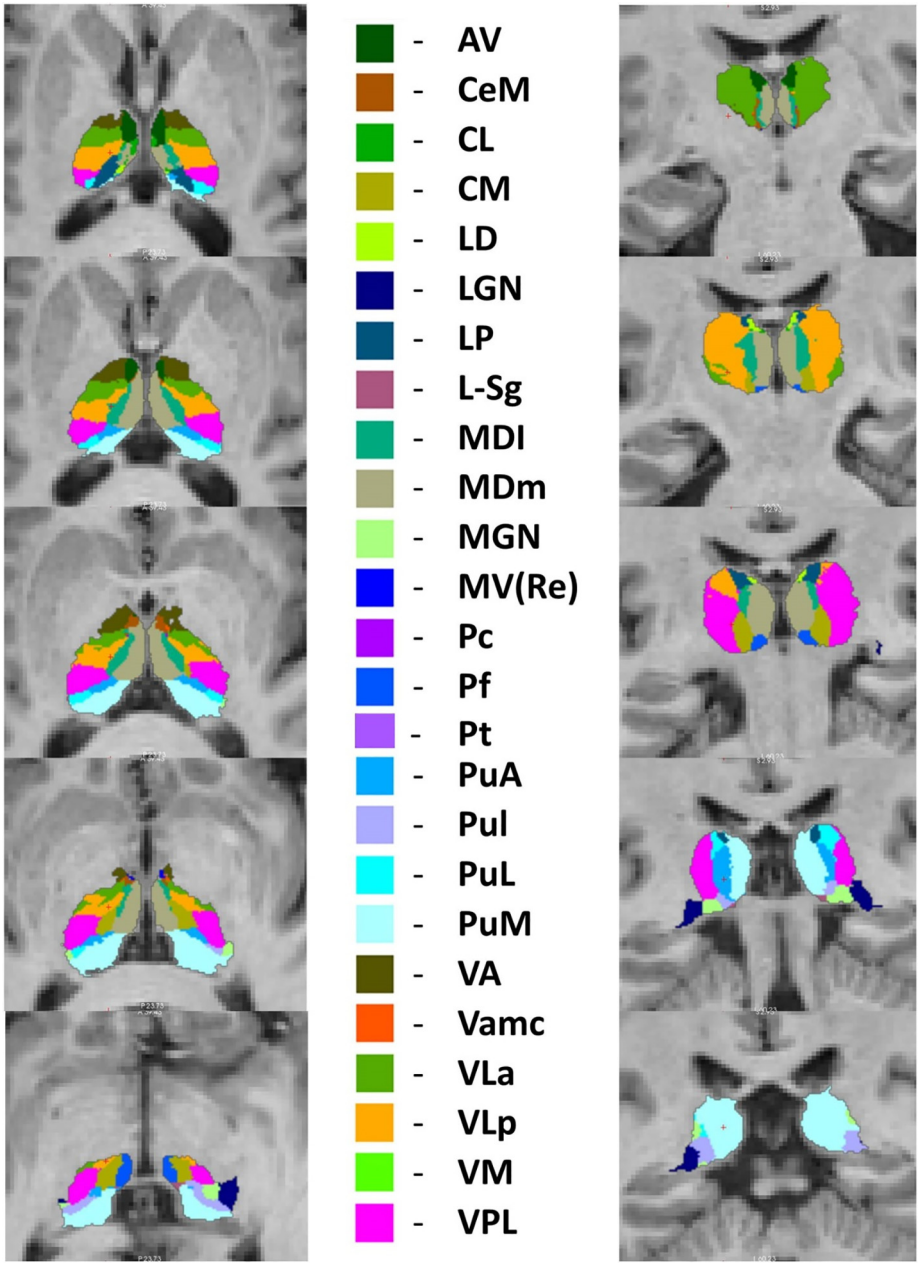

Fig. 1. Atlas-based segmentation of the thalamus; anteroventral (AV), central medial (CeM), central lateral (CL), centromedian (CM), laterodorsal (LD), lateral geniculate (LGN), lateral posterior (LP), limitans/suprageniculate (L-SG), mediodorsal lateral parvocellular (MDl), mediodorsal medial magnocellular (MDm), medial geniculate (MGN), reuniens/medial ventral (MV-re), paracentral (Pc), parafascicular (Pf), pulvinar anterior (PuA), pulvinar inferior (PuI), pulvinar lateral (PuL), pulvinar medial (PuM), ventral anterior (VA), ventral anterior magnocellular (VA mc), ventral lateral anterior (VLa), ventral lateral posterior (VLp), ventromedial (VM), ventral posterolateral (VPL).

3. Results

The four study groups were matched for age, gender, education and handedness. Patients groups were matched for functional disability and site of onset (Table 1).

Thalamic segmentation revealed study-group specific volumetric profiles (Fig. 2). Significant atrophy was identified in the mediodorsal-paratenial-reuniens group of nuclei in all three patient cohorts. Both

Table 1
The demographic and clinical profile of study participants, ECAS: Edinburgh Cognitive ALS Screen, ALSFRS-r: revised ALS functional rating scale, MND-FTD defined by the revised Strong criteria (Strong et al., 2017).

Study Groups	*ALS C9+ n = 12*	*ALS C9- n = 88*	*PLS n = 33*	*HC n = 117*	*p value*
Age (years)	57.25 (16.454)	60.18 (10.311)	60.48 (10.488)	57.38 (11.914)	0.263
Gender (male)	6 (50%)	56 (63.6%)	19 (57.6%)	56 (47.9%)	0.598
Education (years)	12.50 (3.205)	13.58 (3.169)	12.88 (3.380)	14.31 (3.294)	0.053
Handedness (right)	9 (75%)	81 (92%)	29 (87.9%)	109 (93.2%)	0.185
Cognitive impairment on ECAS	7 (58.3%)	19 (21.5%)	8 (24.2%)	n/a	0.023
Comorbid FTD as per the Strong criteria	8 (66.66%)	7 (7.95%)	1 (3.03%)	n/a	< 0.01
Onset (Bulbar)	2 (16.66%)	16 (18.18%)	1 (3.03%)	n/a	0.102
Onset (Limb)	10 (83.33%)	72 (81.81%)	32 (96.96%)	n/a	0.102
ALSFRS-R	36.08 (7.585)	36.69 (7.495)	34.36 (5.337)	n/a	0.272

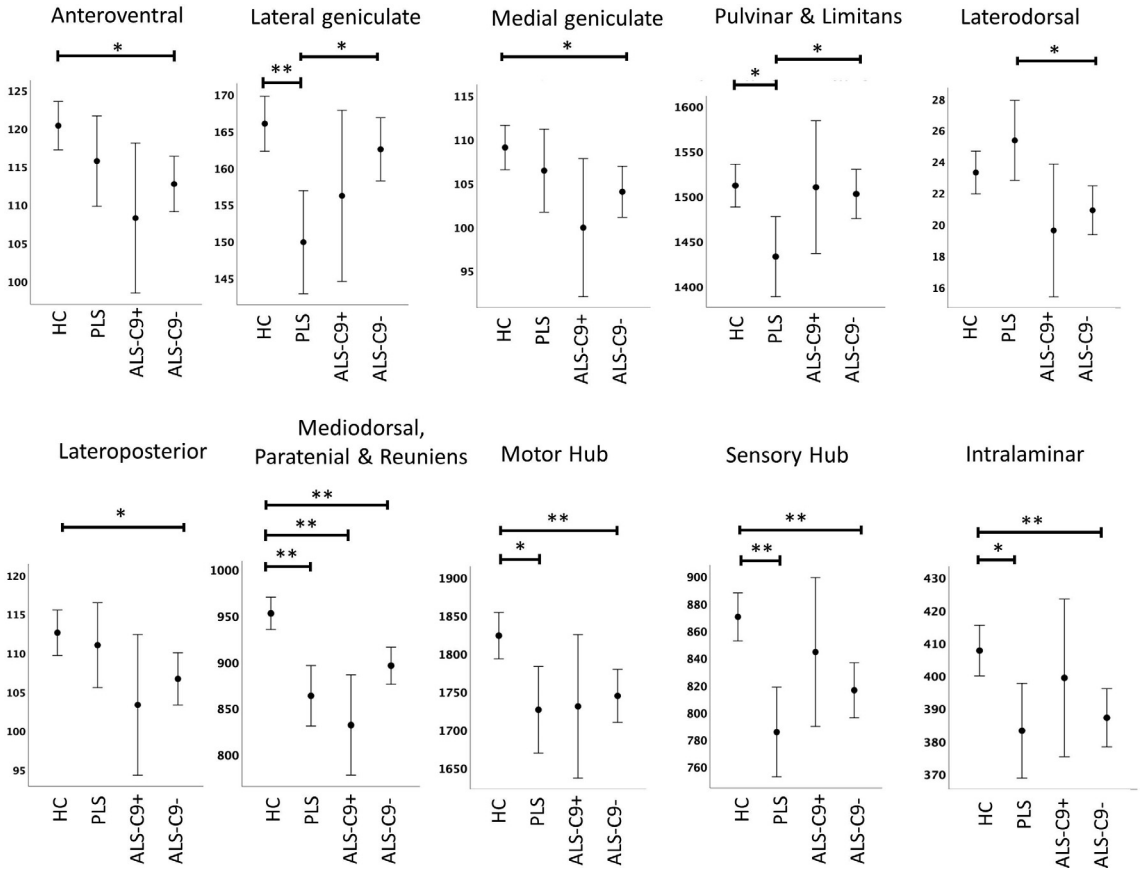

Fig. 2. The volumetric profile of thalamic nuclei in healthy controls (HC), primary lateral sclerosis (PLS), *C9orf72* positive ALS patients (ALS-C9+), and *C9orf72* negative ALS patients (ALS-C9-) based on estimated marginal means adjusted for age, gender, total intracranial volumes (TIV) and education. Error bars represent 95% confidence intervals. Inter-group differences corrected for multiple comparisons are highlighted with asterisks * $p < 0.05$ ** $p < 0.01$.

C9orf72 negative ALS patients and PLS patients exhibited significant volume reductions in motor nuclei, sensory nuclei and intralaminar nuclei. *C9orf72* negative ALS patients showed additional anteroventral, medial geniculate, and lateroposterior changes compared to healthy controls. PLS patients had a distinctive thalamic signature with preferential pulvinar and lateral geniculate compared to healthy controls but also in contrast to *C9orf72* negative ALS patients (Fig. 2). While intergroup differences between hexanucleotide carriers and sporadic ALS patients did not reach significance following FDR corrections, reduced mediodorsal-paratenial-reuniens volumes were observed in hexanucleotide carriers compared to C9orf72 negative ALS patients ($p = 0.085$) (Table 2).

4. Vertex analyses

Vertex analyses also confirmed considerable thalamic atrophy in both ALS cohorts. In C9 + ALS patients strikingly symmetric patterns of atrophy were observed with superior-inferior predominance as well as posterior involvement. Similar patterns were noted in the C9- ALS group compared to healthy controls. The direct comparison of hexanucleotide carrying ALS patients with C9 negative patients revealed asymmetric superior-inferior-posterior atrophy in the right thalamus. Anterior and posterior deformations were observed in PLS compared to C9 negative ALS. Widespread superior, inferior and posterior shape alterations were noted in PLS compared to healthy controls (Fig. 3).

5. Morphometric alterations

Morphometric analyses revealed largely asymmetric changes. Statistically significant right posterolateral atrophy was observed in C9 negative ALS compared to healthy controls at $p < 0.05$ FWE. C9 negative ALS patients exhibited left ventral lateral pathology in comparison to PLS patients at $p < 0.05$ FWE. PLS patients exhibited bilateral posterior density reductions in contrast to healthy controls (Fig. 4).

6. Correlation analyses

Within the patient group (ALS, PLS), we only found a significant association between pulvinar volumes and symptom duration ($r = -0.269$; $p_{FDR} = 0.02$). The association between symptom duration and posterior-lateral geniculate volume did not survive correction for multiple comparisons ($r = -0.208$; $p_{unc} = 0.018$; $p_{FDR} = 0.09$). There were no direct associations between the volumes of motor nuclei and ALS functional rating scale values.

7. Discussion

Our findings indicate phenotype-specific patterns of thalamic degeneration in MND with the preferential involvement of specific nuclei as opposed to global thalamic atrophy. The selective involvement of thalamic nuclei highlights that thalamic pathology in motor neuron diseases is not homogenous; therefore earlier efforts to evaluate the entire structure by volumetric, metabolic, shape or diffusivity measures are likely to have averaged biophysical indices across affected and unaffected regions.

One of the key objectives of the study was to assess thalamic motor nuclei in ALS. The ventral anterior nucleus contributes to planning and initiating movement, while the ventral lateral nucleus plays a role in movement modulation and coordination (Tlamsa and Brumberg, 2010). The majority of ALS imaging studies focus on pyramidal weakness and

Table 2
Subcortical grey matter volumes (mm3) in healthy controls (HC), *C9orf72* positive ALS patients (ALS-C9 +), *C9orf72* negative ALS patients (ALS-C9-) and PLS patients (PLS). Estimated marginal means and standard error are adjusted for age, gender, education and total intracranial volume (TIV). Significant intergroup differences at p < 0.05 after FDR-correction for multiple comparisons are flagged in bold print.

Nuclei	*Study group*	*EMM*	*Standard error*	*C9+ ALS vs HC*	*C9- ALS vs HC*	*PLS vs HC*	*C9+ vs C9-*	*C9+ ALS vs PLS*	*C9- ALS vs PLS*
Anteroventral	HC	120.348	1.606	0.072	**0.011**	0.308	0.502	0.330	0.498
	ALS-C9+	108.247	4.985						
	ALS-C9-	112.701	1.843						
	PLS	115.716	3.004						
Lateral geniculate	HC	166.002	1.903	0.227	0.378	< **0.001**	0.483	0.486	**0.014**
	ALS-C9+	156.178	5.908						
	ALS-C9-	162.525	2.184						
	PLS	149.874	3.560						
Medial geniculate	HC	109.069	1.289	0.085	**0.038**	0.483	0.483	0.300	0.498
	ALS-C9+	99.915	4.000						
	ALS-C9-	104.013	1.479						
	PLS	106.428	2.411						
Pulvinar-limitans	HC	1511.829	12.094	0.963	0.680	**0.011**	0.879	0.178	**0.035**
	ALS-C9+	1510.012	37.536						
	ALS-C9-	1502.542	13.880						
	PLS	1432.716	22.622						
Laterodorsal	HC	23.301	.692	0.212	0.072	0.300	0.666	0.072	**0.017**
	ALS-C9+	19.607	2.148						
	ALS-C9-	20.893	.794						
	PLS	25.344	1.295						
Lateroposterior	HC	112.576	1.480	0.142	**0.037**	0.680	0.605	0.289	0.308
	ALS-C9+	103.304	4.594						
	ALS-C9-	106.652	1.699						
	PLS	110.981	2.769						
Mediodorsal-paratenial-reuniens	HC	952.485	8.870	< **0.001**	< **0.001**	< **0.001**	0.085	0.483	0.207
	ALS-C9+	831.611	27.532						
	ALS-C9-	895.909	10.180						
	PLS	863.272	16.593						
Motor Hub	HC	1823.542	15.441	0.161	**0.007**	**0.014**	0.826	0.950	0.670
	ALS-C9+	1730.548	47.926						
	ALS-C9-	1744.318	17.721						
	PLS	1726.039	28.884						
Sensory Hub	HC	870.109	8.949	0.498	< **0.001**	< **0.001**	0.483	0.165	0.227
	ALS-C9+	844.262	27.777						
	ALS-C9-	816.158	10.271						
	PLS	785.381	16.740						
Intralaminar	HC	407.634	3.941	0.609	**0.007**	**0.017**	0.484	0.407	0.699
	ALS-C9+	399.285	12.231						
	ALS-C9-	387.102	4.523						
	PLS	383.145	7.371						
Whole thalamus	HC	6096.895	43.005	0.098	< **0.001**	< **0.001**	0.774	0.605	0.212
	ALS-C9+	5802.968	133.480						
	ALS-C9-	5852.813	49.356						
	PLS	5698.896	80.445						

evaluate motor cortex, corticospinal tract, brainstem and spinal cord metrics (Querin et al., 2018; Schuster et al., 2016; Omer et al., 2017; Bede et al., 2019). Extrapyramidal motor deficits have been sporadically reported in ALS (Pradat et al., 2009; Desai and Swash, 1999; Christidi et al., 2018; Abidi et al., 2019), but ascertaining extra-pyramidal signs clinically is challenging in the presence of combined upper and lower motor neuron degeneration (Lebouteux et al., 2014). In this study, both *C9orf72* negative ALS patients and PLS patients exhibited significant volume reductions in thalamic motor nuclei. Extrapyramidal features of ALS are relatively under recognised despite case series (Pradat et al., 2009; Desai and Swash, 1999; Williams et al., 1995), gait analyses (Feron et al., 2018), and nuclear medicine studies in both sporadic (Takahashi et al., 1993) and familial cases (Przedborski et al., 1996; O'Dowd et al., 2012). Occupational therapy and physiotherapy interventions in ALS typically focus on pyramidal weakness; spasticity management for UMN dysfunction and fitting orthoses to limbs affected by LMN dysfunction. Impaired gait initiation and impaired postural reflexes however are also likely to contribute to poor mobility and increased fall risk in ALS and may benefit from targeted interventions (Montes et al., 2007; Schell et al., 2019). Extra-pyramidal features of bulbar dysfunction are also poorly characterised; assessments and interventions typically focus on the UMN/LMN aspects of dysarthria and dysphagia (Yunusova et al., 2019). We have not identified direct correlations between ALSFRS-r and motor nucleus volumes in ALS or PLS. This is not unexpected, as ALSFR-r is thought to be disproportionately representative of lower motor neuron degeneration in ALS and may be particularly suboptimal to assess motor disability in PLS (Gordon et al., 2009; Mitsumoto et al., 2020; Finegan et al., 2019b).

We have also identified significant volume reductions in sensory nuclei in both the *C9orf72* negative ALS cohort and in the PLS group. Sensory deficits are seldom evaluated routinely in established ALS and PLS patients, as clinical disability is dominated by relentlessly progressive limb weakness, bulbar impairment and eventually respiratory weakness. Paraesthesiae are often reported by patients but frank nociceptive, proprioceptive or thermoceptive deficits are not characteristic of ALS. Cortical imaging in ALS does not typically identify postcentral gyrus involvement (Schuster et al., 2016), but posterior column degeneration has been previously captured on spinal imaging (Cohen-Adad et al., 2013). Spinal dorsal column degeneration have been reported based on DTI and MT data (Cohen-Adad et al., 2013; Rasoanandrianina et al., 2017) and combined spinal DTI and neurophysiology studies suggest subclinical sensory dysfunction in ALS patients without frank sensory symptoms (Iglesias et al., 2015). There is additional neurophysiological evidence that cerebral sensory

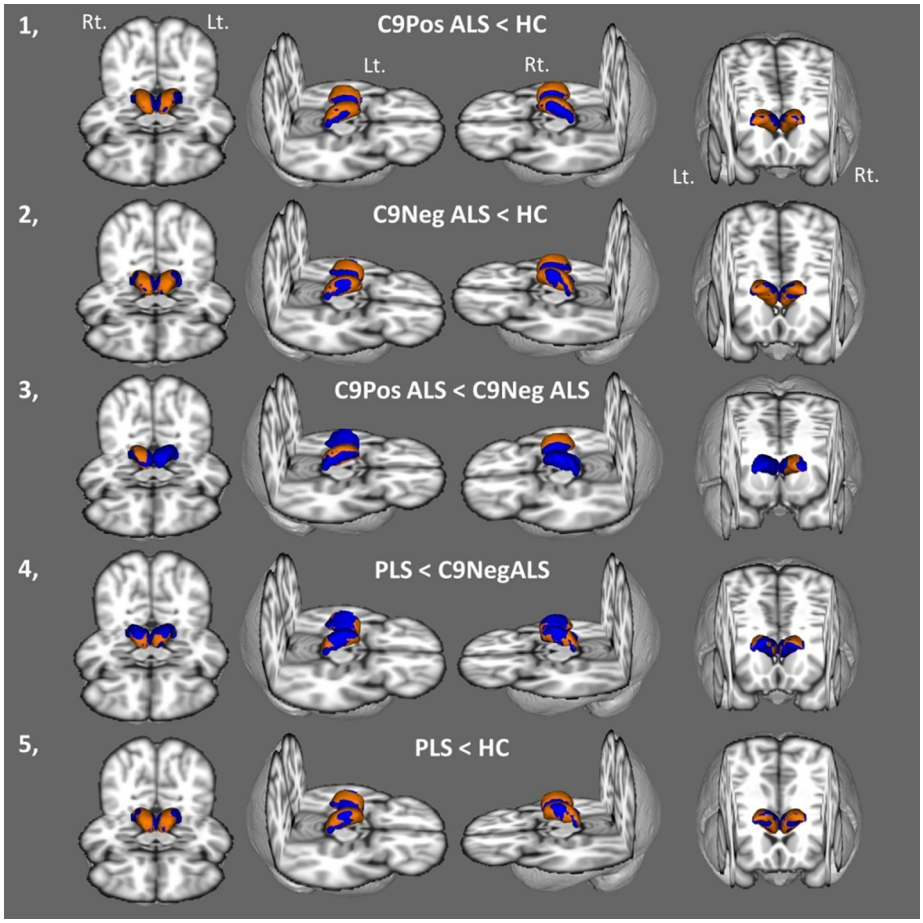

Fig. 3. Shape deformations in C9 positive ALS in comparison to healthy controls (1), C9 negative ALS compared to healthy controls (2), C9 positive ALS compared to C9 negative ALS (3), PLS compared to C9 negative ALS (4), and PLS patients in contrast to healthy controls (5). Average thalamic mesh is shown in blue and surface projected patterns of atrophy are shown in orange colour at $p < 0.05$ corrected for age, gender, education, and TIV. Anterior, superior lateral from the right, superior lateral from the left and posterior inferior views are presented. Rt – right, Lt. – left. (For interpretation of the references to colour in this figure legend, the reader is referred to the web version of this article.)

processing may be affected in ALS (Lule et al., 2010; Nasseroleslami et al., 2019). Our finding of ventral posterolateral and ventral medial thalamus degeneration indicates that sub-clinical sensory deficits are likely to add to the clinical heterogeneity of the condition. Multidisciplinary rehabilitation efforts in ALS should take spinal posterior column and sensory thalamus degeneration into account when assessing gait disturbance and fall risks in ALS (Montes et al., 2007; Schell et al., 2019).

In our study, we identified significant mediodorsal-paratenial-reuniens pathology in both PLS and ALS. Our results suggest that this group of nuclei are affected in ALS irrespective of *C9orf72* status. These nuclei play a physiological role in executive function (Piras et al., 2010; Monchi et al., 2001; Perakyla et al., 2017); memory consolidation (Pergola et al., 2018; Tu et al., 2014), recall (Tu et al., 2014; Pergola et al., 2013). The involvement of thalamic nuclei which mediate cognitive functions mirrors observations of widespread extra-motor cortical involvement in ALS. Both ALS and FTD studies provide ample evidence that thalamic pathology is not unique to *C9orf72* (Westeneng et al., 2016; Bocchetta et al., 2018), and it is also clear that a proportion of *C9orf72* negative sporadic ALS patients fulfil diagnostic criteria for comorbid FTD (Strong et al., 2017). In our C9negative cohort 8% of patients had comorbid FTD and 21% had cognitive impairment based on a disease-specific screening instrument. Our findings support the notion that *C9orf72* is not the sole cause of ALS-associated cognitive impairment and that sporadic cases also exhibit extra-motor grey matter changes and cognitive impairment despite testing negative for a panel of established mutations. Cognitive deficits in ALS are typically linked to extra-motor cortical pathology and frontotemporal white matter alterations, and the contribution of subcortical grey matter degeneration to neuropsychological manifestations is seldom evaluated specifically. Neuropsychological deficits in ALS are thought to be dominated by executive (Abrahams et al., 1995; Elamin et al., 2011) and behavioural dysfunction (Elamin et al., 2017; Burke et al., 2017), but deficits in social cognition (Burke et al., 2016a,b) and memory impairment are also increasingly recognised (Beeldman et al., 2016; Christidi et al., 2017).

Intergroup volumetric differences between hexanucleotide carriers and sporadic ALS patients did not reach significance following FDR corrections in our study, but reduced ($p = 0.085$ FDR) mediodorsal-paratenial-reuniens volumes were observed in hexanucleotide carriers compared to *C9orf72* negative ALS patients. This observation may be a reflection of more widespread cognitive involvement in *C9orf72* carriers in comparison to C9 negative patients which is observed both clinically and on detailed neuropsychological assessment (Byrne et al., 2012; Simón-Sánchez et al., 2012; Patel and Sampson, 2015; Esselin et al., 2020). On vertex analyses however, C9orf72 positive patients exhibited significant superior–inferior shape deformations compared to C9negative patients. GGGGCC hexanucleotide expansions have been specifically linked to pulvinar atrophy in FTD both on imaging (Bocchetta et al., 2020; Lee et al., 2014, 2017) and post mortem (Vatsavayai et al., 2016; Yang et al., 2017). In contrast to observations in FTD, we have not observed preferential pulvinar involvement in our sample of *C9orf72* positive ALS cohort. While the sample size of our *C9orf72* positive cohort is limited, we have observed marked pulvinar atrophy in our PLS cohort who tested negative for repeat expansions. The thalamic profile of our PLS group suggests that pulvinar atrophy is not unique to hexanucleotide repeat expansions carriers in motor neuron diseases.

C9orf72 negative ALS patients also showed significant anteroventral changes compared to healthy controls. The physiological role of the anteroventral nucleus is primarily associated with learning (Warburton et al., 2001) and memory encoding (Stillova et al., 2015). It plays a role

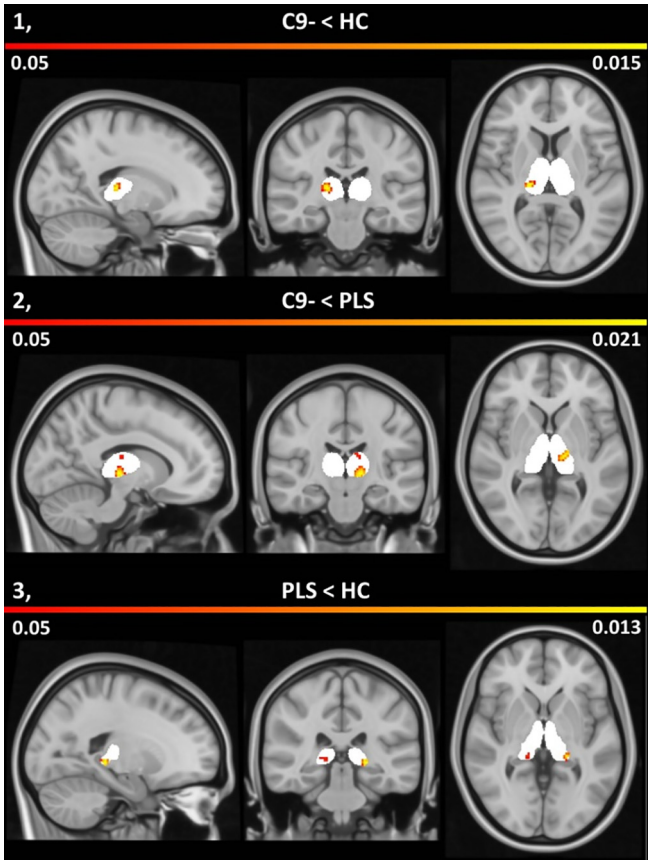

Fig. 4. Patterns of thalamic atrophy in C9 negative ALS in comparison to healthy controls (1), in C9 negative ALS versus PLS (2) and in PLS compared to healthy controls (3). Morphometric changes are shown on an atlas-defined bi-thalamic grey matter mask (white) with corresponding p-values corrected for age, gender, total intracranial volumes and education. The colour bar indicates probability values less than 0.05.

in episodic memory; encoding content and recollection, (Leszczynski and Staudigl, 2016) but has also been linked to emotional processing (Marchand et al., 2014) and executive functions (Ghika-Schmid and Bogousslavsky, 2000). Furthermore, *C9orf72* negative ALS patients exhibited marked pathology in the intralaminar nuclei which mediate a number of cognitive and sensory processes, including arousal, attention, and pain perception (Jang et al., 2014). The involvement of anteroventral and intralaminar nuclei in *C9orf72* negative ALS is consistent with the notion that ALS is a multisystem degenerative condition involving both motor and extra-motor regions. Our findings are also support the growing body of literature that frontotemporal and subcortical grey matter changes are not unique the hexanucleotide repeat carriers in motor neuron disease (Westeneng et al., 2016; Finegan et al., 2019c). The characterisation of the imaging features of a *C9orf72*-negative sporadic ALS cohort is clinically relevant, as they represent the majority of ALS patients presenting to clinics for diagnostic clarification, clinical follow-up and multidisciplinary management. C9negative sporadic ALS patients exhibit the same disease trajectory of relentless motor decline and respiratory compromise within 3–5 years of the diagnosis as those ALS patients carrying established mutations. The involvement of thalamic nuclei mediating cognitive functions therefore highlights the importance of also screening for cognitive deficits in this cohort. Cognitive deficits in ALS have widespread ramifications and may impact on compliance with assistive interventions, adherence to therapy, end-of life decisions, caregiver burden, resource allocation, and pharmacological trial participation (Olney et al., 2005).

Our findings suggest that PLS has a distinctive thalamic signature with preferential pulvinar and lateral geniculate involvement compared to *C9orf72* negative ALS patients. These observations are consistent with the view that PLS has a number of unique, phenotype-specific imaging features, distinct from ALS. The lateral geniculate not only relays retinofugal information to the visual cortex (Wang et al., 2015) it is also thought to contribute to visuospatial filtering and perception (Sherman, 2016). Pulvinar-limitans volume reductions in PLS were more marked than those observed in *C9orf72* negative ALS. Posterior pulvinar thalamic regions play a role in maintaining attention to visual stimuli (Snow et al., 2009), and pulvino-cortical projections are also associated with attention modulation, working memory, and decision making (Jaramillo et al., 2019). The involvement of the motor nuclei, sensory nuclei and the mediodorsal-paratenial-reuniens region in PLS are comparable to the sub-thalamic profile of *C9orf72* negative ALS. Focal pathological changes in sensory thalamus regions have not been previously reported in PLS. The involvement of ventral anterior and ventral lateral nuclei in PLS, which mediate movement initiation and modulation, are relatively novel findings as extrapyramidal dysfunction is not well established in PLS. It is noteworthy that thalamic pathology is thought to contribute to the development pseudobulbar affect (Lauterbach et al., 1994) which has a particularly high prevalence in PLS. Our findings therefore complement the emerging literature of extra-pyramidal and extra-motor deficits in PLS (Clark et al., 2018; de Vries et al., 2019; de Vries et al., 2017).

Post-mortem histopathology findings in ALS are seldom reported in conjunction with ante mortem neuroimaging findings (Irwin et al., 2013; Mahoney et al., 2012) and existing imaging studies have not elaborated on post-mortem thalamus pathology. Studies of pathological TDP-43 patterns in ALS have consistently reported thalamic involvement (Geser et al., 2008), but the vulnerability of specific thalamic nuclei are poorly characterised. Data from large case series (Brettschneider et al., 2013) suggest the preferential involvement of large thalamic relay neurons projecting to layer IV of the neocortex which is associated with Stage 2 of a corticofugal pTDP-43 model (Braak et al., 2013). Few post-mortem studies have specifically evaluated thalamic changes in the ALS spectrum and many of these are case reports or case-series (Gamez et al., 2008). The paucity of post mortem thalamus studies in ALS is in sharp contrast to FTD, where thalamic changes have been comprehensively evaluated in patients stratified for clinical phenotypes (De Reuck et al., 2014) and specific genotypes (Vatsavayai et al., 2016; Yang et al., 2017). Presymptomatic imaging studies have consistently highlighted thalamic pathology before disease manifestation (Lee et al., 2017; Popuri et al., 2018; Bertrand et al., 2018; Papma et al., 2017) but there is a lack of consensus regarding propagation biology in ALS. While the controversy around corticofugal versus corticopetal spread persists, transneuronal processes and microglial inflammation are established mechanisms of disease propagation in ALS. Imaging studies in ALS have played a limited role in clarifying underlying molecular processes, but they have repeatedly noted the concomitant degeneration of structurally or functionally interconnected brain regions (Verstraete et al., 2013; Bak and Chandran, 2012). As the thalamus relays a multitude of corticoefferent and corticoafferent connections, its selective involvement in ALS mirrors the widespread cerebral and spinal cord alterations associated with the condition.

Global thalamus pathology has been previously investigated in ALS by a multitude of techniques including VBM, total volumes, texture analysis, spectroscopy, TBSS, PET, fMRI and parcellation based on cortical connectivity. In this study we have primarily focused on the volumetric characterisation of thalamic nuclei, but supplementary vertex and morphometric analyses were also carried out. Relatively limited concordance was identified between regional volume reductions, shape deformations and morphometric changes. While anatomical segmentation revealed selective nuclear atrophy, vertex analyses only showcased overall shape deformation without providing specific information on which nuclei were driving these changes. This

highlights the relative limitation of evaluating surface-projected vertex changes alone in structures which consist of multiple sub-regions with potentially varying vulnerability to ALS. Our findings also highlight the limitations of assessing total thalamic volumes in MND phenotypes. Total thalamus volume reduction did not reach significance in the *C9orf72* positive cohort compared to controls, but the assessment of mediodorsal-paratenial nuclei revealed marked volume reductions in hexanucleotide carriers. Furthermore, while total thalamus volumes were similarly reduced in C9negative ALS and PLS, their nuclear profiles are distinctly different; the laterodorsal nuclei were preferentially affected in C9negative ALS and the pulvinar region in PLS.

This study has a number of limitations. Consistent with the population-based incidence of *C9orf72* in ALS, the cohort size of C9 + ALS group is limited which precludes conclusive genotype-associated observations. The inclusion of a non-MND disease-control group with an alternative neurodegenerative diagnosis, such as AD or FTD would have supported the specificity of our thalamic findings to ALS and PLS. We have focused on descriptive analyses and not explored direct clinico-radiological correlations between neuropsychological measures and imaging findings (Verstraete et al., 2015). Cognitive functions and behavioural regulation are mediated through function-specific multi-synaptic cortico-basal circuits (O'Callaghan et al., 2013) and therefore seeking direct associations between clinical measures and focal thalamic indices would overlook the contribution of other white and grey matter components to clinical performance. Post mortem histopathology data or ex-vivo MRI would have provided important validation for the radiological observations made in vivo (Bede, 2019). A limitation of our supplementary morphometric analysis is that it used labels from a different atlas than the one utilised for anatomical segmentation. Finally, while our data provides a snapshot of thalamic alterations in ALS, a robust multi-timepoint design would have provided crucial longitudinal insights (Chipika et al., 2019; Schuster et al., 2015). Notwithstanding these limitations, our data provide evidence of focal thalamic involvement in ALS and PLS and demonstrate the utility of appraising thalamic nuclei individually instead of evaluating overall thalamic changes.

8. Conclusions

We have detected phenotype-specific patterns of focal thalamic pathology in ALS and PLS. The characterisation of thalamic pathology allows the identification of the most vulnerable group of nuclei, the measures of which are superior biomarkers candidates than indices of the entire structure. The pathology of thalamic nuclei mediating sensory, cognitive and behavioural functions support the conceptualisation of ALS and PLS as multi-system conditions. The thalamic profiles of ALS and PLS provide anatomical evidence of extra-pyramidal motor and sensory involvement in these conditions.

CRediT authorship contribution statement

Rangariroyashe H. Chipika: Writing - original draft, Investigation. **Eoin Finegan:** Investigation. **Stacey Li Hi Shing:** Investigation. **Mary C. McKenna:** Investigation. **Foteini Christidi:** Investigation. **Kai Ming Chang:** Investigation. **Mark A. Doherty:** Investigation. **Jennifer C. Hengeveld:** Investigation. **Alice Vajda:** Investigation. **Niall Pender:** Investigation. **Siobhan Hutchinson:** Investigation. **Colette Donaghy:** Investigation. **Russell L. McLaughlin:** Investigation. **Orla Hardiman:** Investigation. **Peter Bede:** Conceptualization, Funding acquisition, Investigation, Writing - review & editing.

Acknowledgements

We gratefully acknowledge all the motor neuron disease patients and controls who have participated in this research study. Without their generosity this study would have not been possible. Peter Bede and the computational neuroimaging group are supported by the Health Research Board (HRB EIA-2017-019), the EU Joint Programme – Neurodegenerative Disease Research (JPND), the Andrew Lydon scholarship, the Irish Institute of Clinical Neuroscience (IICN), the Iris O'Brien Foundation, the Research Motor Neuron (RMN-Ireland) Foundation and the Irish Motor Neuron Disease Association (IMNDA). Russell L McLaughlin is supported by the Motor Neurone Disease Association (957-799) and Science Foundation Ireland (17/CDA/4737). Mark A Doherty is supported by Science Foundation Ireland (15/SPP/3244). Foteini Christidi is supported by the EU-IKY Scholarship Program (European Social Fund-ESF), the Greek "Reinforcement of Postdoctoral Researchers" grant (5033021) of the "Human Resources Development Program, Education and Lifelong Learning" of the National Strategic Reference Framework (NSRF 2014-2020). The sponsors of this study had no direct role in the design, analyses, presentation of this work or the decision to submit these findings for publication.

References

Abidi, M., et al., 2019. Adaptive functional reorganization in amyotrophic lateral sclerosis: coexisting degenerative and compensatory changes. Eur. J. Neurol.
Abrahams, S., et al., 1995. Cognitive deficits in non-demented amyotrophic lateral sclerosis patients: a neuropsychological investigation. J. Neurol. Sci. 129 (Suppl), 54–55.
Abrahams, S., et al., 2014. Screening for cognition and behaviour changes in ALS. Amyotroph. Lateral Scler. Frontotemporal Degener. 15 (1–2), 9–14.
Bak, T.H., Chandran, S., 2012. What wires together dies together: verbs, actions and neurodegeneration in motor neuron disease. Cortex 48 (7), 936–944.
Bede, P., et al., 2013b. Basal ganglia involvement in amyotrophic lateral sclerosis. Neurology 81 (24), 2107–2115.
Bede, P., et al., 2013a. Multiparametric MRI study of ALS stratified for the C9orf72 genotype. Neurology 81 (4), 361–369.
Bede, P., et al., 2018. Connectivity-based characterisation of subcortical grey matter pathology in frontotemporal dementia and ALS: a multimodal neuroimaging study. Brain Imaging Behav. 12 (6), 1696–1707.
Bede, P., 2019. The histological correlates of imaging metrics: postmortem validation of in vivo findings. Amyotroph Lateral Scler. Frontotemporal Degener. 20 (7–8), 457–460.
Bede, P., et al., 2019. Brainstem pathology in amyotrophic lateral sclerosis and primary lateral sclerosis: a longitudinal neuroimaging study. Neuroimage Clin 24, 102054.
Beeldman, E., et al., 2016. The cognitive profile of ALS: a systematic review and meta-analysis update. J. Neurol. Neurosurg. Psychiatry 87 (6), 611–619.
Behrens, T.E., et al., 2003. Non-invasive mapping of connections between human thalamus and cortex using diffusion imaging. Nat. Neurosci. 6 (7), 750–757.
Bertrand, A., et al., 2018. Early cognitive, structural, and microstructural changes in presymptomatic C9orf72 carriers younger than 40 years. JAMA Neurol. 75 (2), 236–245.
Blackshaw, S., et al., 2010. Molecular pathways controlling development of thalamus and hypothalamus: from neural specification to circuit formation. J. Neurosci. 30 (45), 14925–14930.
Bocchetta, M., et al., 2018. Thalamic atrophy in frontotemporal dementia - Not just a C9orf72 problem. Neuroimage Clin. 18, 675–681.
Bocchetta, M., et al., 2020. Thalamic nuclei in frontotemporal dementia: Mediodorsal nucleus involvement is universal but pulvinar atrophy is unique to C9orf72. Hum. Brain Mapp. 41 (4), 1006–1016.
Bosch-Bouju, C., Hyland, B.I., Parr-Brownlie, L.C., 2013. Motor thalamus integration of cortical, cerebellar and basal ganglia information: implications for normal and parkinsonian conditions. Front. Comput. Neurosci. 7, 163.
Braak, H., et al., 2013. Amyotrophic lateral sclerosis–a model of corticofugal axonal spread. Nat. Rev. Neurol. 9 (12), 708–714.
Brettschneider, J., et al., 2013. Stages of pTDP-43 pathology in amyotrophic lateral sclerosis. Ann. Neurol. 74 (1), 20–38.
Brooks, B.R., et al., 2000. El Escorial revisited: revised criteria for the diagnosis of amyotrophic lateral sclerosis. Amyotroph. Lateral Scler. Other Motor Neuron Disord. 1 (5), 293–299.
Burke, T., et al., 2016a. Measurement of social cognition in amyotrophic lateral sclerosis: a population based study. PLoS One 11 (8), e0160850.
Burke, T., et al., 2016b. Discordant performance on the 'Reading the Mind in the Eyes' Test, based on disease onset in amyotrophic lateral sclerosis. Amyotroph Lateral Scler. Frontotemporal. Degener. 1–6.
Burke, T., et al., 2017. A Cross-sectional population-based investigation into behavioral change in amyotrophic lateral sclerosis: subphenotypes, staging, cognitive predictors, and survival. Ann. Clin. Transl. Neurol. 4 (5), 305–317.
Byrne, S., et al., 2012. Cognitive and clinical characteristics of patients with amyotrophic lateral sclerosis carrying a C9orf72 repeat expansion: a population-based cohort study. Lancet Neurol. 11 (3), 232–240.
Cedarbaum, J.M., et al., 1999. The ALSFRS-R: a revised ALS functional rating scale that incorporates assessments of respiratory function. BDNF ALS Study Group (Phase III). J. Neurol. Sci. 169 (1–2), 13–21.

Chang, J.L., et al., 2005. A voxel-based morphometry study of patterns of brain atrophy in ALS and ALS/FTLD. Neurology 65 (1), 75–80.
Chipika, R.H., et al., 2019. Tracking a fast-moving disease: longitudinal markers, monitoring, and clinical trial endpoints in ALS. Front. Neurol. 10, 229.
Christidi, F., et al., 2017. Memory-related white matter tract integrity in amyotrophic lateral sclerosis: an advanced neuroimaging and neuropsychological study. Neurobiol. Aging 49, 69–78.
Christidi, F., et al., 2018. Clinical and radiological markers of extra-motor deficits in amyotrophic lateral sclerosis. Front. Neurol. 9, 1005.
Cistaro, A., et al., 2014. The metabolic signature of C9ORF72-related ALS: FDG PET comparison with nonmutated patients. Eur. J. Nucl. Med. Mol. Imaging.
Clark, M.G., et al., 2018. Loss of functional connectivity is an early imaging marker in primary lateral sclerosis. Amyotroph. Lateral Scler. Frontotemporal Degener. 19 (7–8), 562–569.
Cohen-Adad, J., et al., 2013. Involvement of spinal sensory pathway in ALS and specificity of cord atrophy to lower motor neuron degeneration. Amyotroph Lateral Scler. Frontotemporal. Degener. 14 (1), 30–38.
De Reuck, J.L., et al., 2014. Iron deposits in post-mortem brains of patients with neurodegenerative and cerebrovascular diseases: a semi-quantitative 7.0 T magnetic resonance imaging study. Eur. J. Neurol. 21 (7), 1026–1031.
de Vries, B.S., et al., 2017. A case series of PLS patients with frontotemporal dementia and overview of the literature. Amyotrophic Lateral Scler. Frontotemporal Degen. 18 (7–8), 534–548.
de Vries, B.S., et al., 2019. A neuropsychological and behavioral study of PLS. Amyotroph. Lateral Scler. Frontotemporal Degener. 20 (5–6), 376–384.
Desai, J., Swash, M., 1999. Extrapyramidal involvement in amyotrophic lateral sclerosis: backward falls and retropulsion. J. Neurol. Neurosurg. Psychiatry 67 (2), 214–216.
Desikan, R.S., et al., 2006. An automated labeling system for subdividing the human cerebral cortex on MRI scans into gyral based regions of interest. Neuroimage 31 (3), 968–980.
Elamin, M., et al., 2011. Executive dysfunction is a negative prognostic indicator in patients with ALS without dementia. Neurology 76 (14), 1263–1269.
Elamin, M., et al., 2017. Identifying behavioural changes in ALS: Validation of the Beaumont Behavioural Inventory (BBI). Amyotroph Lateral Scler. Frontotemporal. Degener. 18 (1–2), 68–73.
Esselin, F., et al., 2020. Clinical phenotype and inheritance in patients with C9ORF72 hexanucleotide repeat expansion: results from a large french cohort. Front. Neurosci. 14, 316.
Feron, M., et al., 2018. Extrapyramidal deficits in ALS: a combined biomechanical and neuroimaging study. J. Neurol. 265 (9), 2125–2136.
Finegan, E., et al., 2019a. The clinical and radiological profile of primary lateral sclerosis: a population-based study. J. Neurol. 266 (11), 2718–2733.
Finegan, E., et al., 2019b. Primary lateral sclerosis: a distinct entity or part of the ALS spectrum? Amyotroph Lateral Scler. Frontotemporal. Degener. 20 (3–4), 133–145.
Finegan, E., et al., 2019c. Widespread subcortical grey matter degeneration in primary lateral sclerosis: a multimodal imaging study with genetic profiling. Neuroimage Clin. 24, 102089.
Floeter, M.K., et al., 2016. Longitudinal imaging in C9orf72 mutation carriers: Relationship to phenotype. Neuroimage Clin. 12, 1035–1043.
Floeter, M.K., et al., 2018. Longitudinal diffusion imaging across the C9orf72 clinical spectrum. J. Neurol. Neurosurg. Psychiatry 89 (1), 53–60.
Floeter, M.K., Mills, R., 2009. Progression in primary lateral sclerosis: a prospective analysis. Amyotrophic Lateral Sclerosis 10 (5–6), 339–346.
Gamez, J., et al., 2008. Chorea-ballism associated with familial amyotrophic lateral sclerosis. A clinical, genetic, and neuropathological study. Mov. Disord. 23 (3), 434–438.
Geser, F., et al., 2008. Evidence of multisystem disorder in whole-brain map of pathological TDP-43 in amyotrophic lateral sclerosis. Arch. Neurol. 65 (5), 636–641.
Ghika-Schmid, F., Bogousslavsky, J., 2000. The acute behavioral syndrome of anterior thalamic infarction: a prospective study of 12 cases. Ann. Neurol. 48 (2), 220–227.
Gordon, P.H., et al., 2006. The natural history of primary lateral sclerosis. Neurology 66 (5), 647–653.
Gordon, P.H., et al., 2009. Clinical features that distinguish PLS, upper motor neuron-dominant ALS, and typical ALS. Neurology 72 (22), 1948–1952.
Iglesias, C., et al., 2015. Electrophysiological and spinal imaging evidences for sensory dysfunction in amyotrophic lateral sclerosis. BMJ Open 5 (2), e007659.
Iglesias, J.E., et al., 2018. A probabilistic atlas of the human thalamic nuclei combining ex vivo MRI and histology. Neuroimage 183, 314–326.
Irwin, D.J., et al., 2013. Cognitive decline and reduced survival in C9orf72 expansion frontotemporal degeneration and amyotrophic lateral sclerosis. J. Neurol. Neurosurg. Psychiatry 84 (2), 163–169.
Jang, S.H., Lim, H.W., Yeo, S.S., 2014. The neural connectivity of the intralaminar thalamic nuclei in the human brain: a diffusion tensor tractography study. Neurosci. Lett. 579, 140–144.
Jaramillo, J., Mejias, J.F., Wang, X.J., 2019. Engagement of pulvino-cortical feedforward and feedback pathways in cognitive computations. Neuron 101 (2), 321–336.e9.
Jenkinson, M., et al., 2002. Improved optimization for the robust and accurate linear registration and motion correction of brain images. Neuroimage 17 (2), 825–841.
Johansen-Berg, H., et al., 2005. Functional-anatomical validation and individual variation of diffusion tractography-based segmentation of the human thalamus. Cereb. Cortex 15 (1), 31–39.
Kenna, K.P., et al., 2013. Delineating the genetic heterogeneity of ALS using targeted high-throughput sequencing. J. Med. Genet.
Kiernan, M.C., et al., 2011. Amyotrophic lateral sclerosis. Lancet 377 (9769), 942–955.
Klebe, S., Stevanin, G., Depienne, C., 2015. Clinical and genetic heterogeneity in hereditary spastic paraplegias: from SPG1 to SPG72 and still counting. Rev. Neurol. (Paris) 171 (6–7), 505–530.
Lauterbach, E.C., et al., 1994. Serotonin responsive and nonresponsive diurnal depressive mood disorders and pathological affect in thalamic infarct associated with myoclonus and blepharospasm. Biol. Psychiatry 35 (7), 488–490.
Le Forestier, N., Meininger, V., 2009. Primary lateral sclerosis: the era of international diagnosis criteria. Rev. Neurol. (Paris) 165 (5), 415–429.
Lebouteux, M.V., et al., 2014. Revisiting the spectrum of lower motor neuron diseases with snake eyes appearance on magnetic resonance imaging. Eur. J. Neurol. 21 (9), 1233–1241.
Lee, S.E., et al., 2014. Altered network connectivity in frontotemporal dementia with C9orf72 hexanucleotide repeat expansion. Brain 137 (Pt 11), 3047–3060.
Lee, S.E., et al., 2017. Network degeneration and dysfunction in presymptomatic C9ORF72 expansion carriers. Neuroimage Clin. 14, 286–297.
Leszczynski, M., Staudigl, T., 2016. Memory-guided attention in the anterior thalamus. Neurosci. Biobehav. Rev. 66, 163–165.
Lule, D., et al., 2010. Neuroimaging of multimodal sensory stimulation in amyotrophic lateral sclerosis. J. Neurol. Neurosurg. Psychiatry 81 (8), 899–906.
Machts, J., et al., 2015. Basal ganglia pathology in ALS is associated with neuropsychological deficits. Neurology 85 (15), 1301–1309.
Mahoney, C.J., et al., 2012. Frontotemporal dementia with the C9ORF72 hexanucleotide repeat expansion: clinical, neuroanatomical and neuropathological features. Brain 135 (Pt 3), 736–750.
Mahoney, C.J., et al., 2012. Longitudinal neuroimaging and neuropsychological profiles of frontotemporal dementia with C9ORF72 expansions. Alzheimers Res. Ther. 4 (5), 41.
Marchand, A., et al., 2014. A role for anterior thalamic nuclei in contextual fear memory. Brain Struct. Funct. 219 (5), 1575–1586.
Menke, R.A., et al., 2014. Widespread grey matter pathology dominates the longitudinal cerebral MRI and clinical landscape of amyotrophic lateral sclerosis. Brain 137 (Pt 9), 2546–2555.
Mitsumoto, H., et al., 2020. Primary lateral sclerosis (PLS) functional rating scale: PLS-specific clinimetric scale. Muscle Nerve 61 (2), 163–172.
Monchi, O., et al., 2001. Wisconsin Card Sorting revisited: distinct neural circuits participating in different stages of the task identified by event-related functional magnetic resonance imaging. J. Neurosci. 21 (19), 7733–7741.
Montes, J., et al., 2007. The timed up and go test: predicting falls in ALS. Amyotroph. Lateral Scler. 8 (5), 292–295.
Nasseroleslami, B., et al., 2019. Characteristic increases in EEG connectivity correlate with changes of structural MRI in amyotrophic lateral sclerosis. Cereb. Cortex 29 (1), 27–41.
Neumann, M., et al., 2006. Ubiquitinated TDP-43 in frontotemporal lobar degeneration and amyotrophic lateral sclerosis. Science 314 (5796), 130–133.
Nichols, T.E., Holmes, A.P., 2002. Nonparametric permutation tests for functional neuroimaging: a primer with examples. Hum. Brain Mapp. 15 (1), 1–25.
O'Callaghan, C., Bertoux, M., Hornberger, M., 2013. Beyond and below the cortex: the contribution of striatal dysfunction to cognition and behaviour in neurodegeneration. J. Neurol. Neurosurg. Psychiatry.
O'Dowd, S., et al., 2012. C9ORF72 expansion in amyotrophic lateral sclerosis/frontotemporal dementia also causes parkinsonism. Mov. Disord. 27 (8), 1072–1074.
Olney, R.K., et al., 2005. The effects of executive and behavioral dysfunction on the course of ALS. Neurology 65 (11), 1774–1777.
Omer, T., et al., 2017. Neuroimaging patterns along the ALS-FTD spectrum: a multiparametric imaging study. Amyotroph. Lateral Scler. Frontotemporal. Degener. 18 (7–8), 611–623.
Papma, J.M., et al., 2017. Cognition and gray and white matter characteristics of presymptomatic C9orf72 repeat expansion. Neurology 89 (12), 1256–1264.
Patel, A.N., Sampson, J.B., 2015. Cognitive profile of C9orf72 in frontotemporal dementia and amyotrophic lateral sclerosis. Curr. Neurol. Neurosci. Rep. 15 (9), 59.
Patenaude, B., et al., 2011. A Bayesian model of shape and appearance for subcortical brain segmentation. Neuroimage 56 (3), 907–922.
Perakyla, J., et al., 2017. Causal evidence from humans for the role of mediodorsal nucleus of the thalamus in working memory. J. Cogn. Neurosci. 29 (12), 2090–2102.
Pergola, G., et al., 2013. The role of the thalamic nuclei in recognition memory accompanied by recall during encoding and retrieval: an fMRI study. Neuroimage 74, 195–208.
Pergola, G., et al., 2018. The regulatory role of the human mediodorsal thalamus. Trends Cogn. Sci. 22 (11), 1011–1025.
Pinto-Grau, M., et al., 2017. Screening for cognitive dysfunction in ALS: validation of the Edinburgh Cognitive and Behavioural ALS Screen (ECAS) using age and education adjusted normative data. Amyotroph Lateral Scler. Frontotemporal Degener. 18 (1–2), 99–106.
Piras, F., Caltagirone, C., Spalletta, G., 2010. Working memory performance and thalamus microstructure in healthy subjects. Neuroscience 171 (2), 496–505.
Popuri, K., et al., 2018. Gray matter changes in asymptomatic C9orf72 and GRN mutation carriers. Neuroimage Clin. 18, 591–598.
Pradat, P.-F., et al., 2009. Extrapyramidal stiffness in patients with amyotrophic lateral sclerosis. Mov. Disord. 24 (14), 2143–2148.
Project MinE: study design and pilot analyses of a large-scale whole-genome sequencing study in amyotrophic lateral sclerosis. Eur J Hum Genet, 2018. 26(10): p. 1537-1546.
Przedborski, S., et al., 1996. Nigrostriatal dopaminergic function in familial amyotrophic lateral sclerosis patients with and without copper/zinc superoxide dismutase mutations. Neurology 47 (6), 1546–1551.
Querin, G., et al., 2018. Multimodal spinal cord MRI offers accurate diagnostic classification in ALS. J. Neurol. Neurosurg. Psychiatry 89 (11), 1220–1221.
Rasoanandrianina, H., et al., 2017. Region-specific impairment of the cervical spinal cord (SC) in amyotrophic lateral sclerosis: a preliminary study using SC templates and

quantitative MRI (diffusion tensor imaging/inhomogeneous magnetization transfer). NMR Biomed. 30 (12).
Sangari, S., et al., 2018. Abnormal cortical brain integration of somatosensory afferents in ALS. Clin. Neurophysiol. 129 (4), 874–884.
Schell, W.E., Mar, V.S., Da Silva, C.P., 2019. Correlation of falls in patients with Amyotrophic Lateral Sclerosis with objective measures of balance, strength, and spasticity. NeuroRehabilitation 44 (1), 85–93.
Schmahmann, J.D., 2003. Vascular syndromes of the thalamus. Stroke 34 (9), 2264–2278.
Schuster, C., et al., 2015. Presymptomatic and longitudinal neuroimaging in neurodegeneration–from snapshots to motion picture: a systematic review. J. Neurol. Neurosurg. Psychiatry 86 (10), 1089–1096.
Schuster, C., et al., 2016. The segmental diffusivity profile of amyotrophic lateral sclerosis associated white matter degeneration. Eur. J. Neurol. 23 (8), 1361–1371.
Schuster, C., Hardiman, O., Bede, P., 2016. Development of an Automated MRI-based diagnostic protocol for amyotrophic lateral sclerosis using disease-specific pathognomonic features: a quantitative disease-state classification study. PLoS One 11 (12), e0167331.
Sharma, K.R., et al., 2011. 1H MRS of basal ganglia and thalamus in amyotrophic lateral sclerosis. NMR Biomed. 24 (10), 1270–1276.
Sherman, S.M., 2016. Thalamus plays a central role in ongoing cortical functioning. Nat. Neurosci. 19 (4), 533–541.
Simón-Sánchez, J., et al., 2012. The clinical and pathological phenotype of C9ORF72 hexanucleotide repeat expansions. Brain 135 (Pt 3), 723–735.
Smith, S.M., 2002. Fast robust automated brain extraction. Hum. Brain Mapp. 17 (3), 143–155.
Snow, J.C., et al., 2009. Impaired attentional selection following lesions to human pulvinar: evidence for homology between human and monkey. Proc. Natl. Acad. Sci. U.S.A. 106 (10), 4054–4059.
Stillova, K., et al., 2015. The role of anterior nuclei of the thalamus: a subcortical gate in memory processing: an intracerebral recording study. PLoS One 10 (11), e0140778.
Strong, M.J., et al., 2017. Amyotrophic lateral sclerosis - frontotemporal spectrum disorder (ALS-FTSD): revised diagnostic criteria. Amyotroph Lateral Scler. Frontotemporal Degener. 18 (3–4), 153–174.
Takahashi, H., et al., 1993. Evidence for a dopaminergic deficit in sporadic amyotrophic lateral sclerosis on positron emission scanning. Lancet 342 (8878), 1016–1018.
Tao, Q.Q., Wei, Q., Wu, Z.Y., 2018. Sensory nerve disturbance in amyotrophic lateral sclerosis. Life Sci. 203, 242–245.
Tlamsa, A.P., Brumberg, J.C., 2010. Organization and morphology of thalamocortical neurons of mouse ventral lateral thalamus. Somatosens. Mot. Res. 27 (1), 34–43.
Tu, S., et al., 2014. Accelerated forgetting of contextual details due to focal medio-dorsal thalamic lesion. Front. Behav. Neurosci. 8, 320.
Tu, S., et al., 2018. Regional thalamic MRI as a marker of widespread cortical pathology and progressive frontotemporal involvement in amyotrophic lateral sclerosis. J. Neurol. Neurosurg. Psychiatry 89 (12), 1250–1258.
Vatsavayai, S.C., et al., 2016. Timing and significance of pathological features in C9orf72 expansion-associated frontotemporal dementia. Brain 139 (Pt 12), 3202–3216.
Verstraete, E., et al., 2013. Structural brain network imaging shows expanding disconnection of the motor system in amyotrophic lateral sclerosis. Hum. Brain Mapp.
Verstraete, E., et al., 2015. Mind the gap: the mismatch between clinical and imaging metrics in ALS. Amyotroph Lateral Scler. Frontotemporal Degener. 16 (7–8), 524–529.
Wang, J., et al., 2015. Automatic segmentation of the lateral geniculate nucleus: application to control and glaucoma patients. J. Neurosci. Methods 255, 104–114.
Warburton, E.C., et al., 2001. The conjoint importance of the hippocampus and anterior thalamic nuclei for allocentric spatial learning: evidence from a disconnection study in the rat. J. Neurosci. 21 (18), 7323–7330.
Westeneng, H.J., et al., 2015. Subcortical structures in amyotrophic lateral sclerosis. Neurobiol. Aging 36 (2), 1075–1082.
Westeneng, H.J., et al., 2016. Widespread structural brain involvement in ALS is not limited to the C9orf72 repeat expansion. J. Neurol. Neurosurg. Psychiatry 87 (12), 1354–1360.
Williams, T.L., et al., 1995. Parkinsonism in motor neuron disease: case report and literature review. Acta Neuropathol. 89 (3), 275–283.
Winkler, A.M., et al., 2014. Permutation inference for the general linear model. Neuroimage 92, 381–397.
Yang, Y., et al., 2017. von Economo neuron density and thalamus volumes in behavioral deficits in frontotemporal dementia cases with and without a C9ORF72 repeat expansion. J. Alzheimers Dis. 58 (3), 701–709.
Yunusova, Y., et al., 2019. Clinical measures of bulbar dysfunction in ALS. Front. Neurol. 10, 106.
Zhang, J.Q., et al., 2017. Differential impairment of thalamocortical structural connectivity in amyotrophic lateral sclerosis. CNS Neurosci. Ther. 23 (2), 155–161.
Zhang, Y., Brady, M., Smith, S., 2001. Segmentation of brain MR images through a hidden Markov random field model and the expectation-maximization algorithm. IEEE Trans. Med. Imaging 20 (1), 45–57.

Glossary

ALS: Amyotrophic lateral sclerosis
ALS T1: ALS cohort at the first timepoint
ALS T2: ALS cohort at the second timepoint
ANCOVA: Analysis of covariance,
AV: antero-ventral nuclei
BG: Basal ganglia
C9orf72: chromosome 9 open reading frame 72
CeM: central medial nucleus
CL: central lateral nucleus
CM: centromedian nucleus
CST: Corticospinal tract
Cr: creatine-phosphocreatine
DTI: diffusion tensor imaging
EMM: Estimated marginal mean
EPI: Echo-planar imaging
FTD: Frontotemporal dementia
FOV: Field-of-view
FSL: FMRIB Software Library
FWE: Familywise error
GM: Grey matter
HC: Healthy control
IR-SPGR: Inversion Recovery prepared Spoiled Gradient Recalled echo
LD: latero-dorsal nuclei
LGN: lateral geniculate
LMN: Lower motor neuron
LP: lateral posterior nuclei
L-SG: limitans/suprageniculate nuclei
M: Mean
MDI: mediodorsal lateral parvocellular nuclei
MDm: mediodorsal medial magnocellular nuclei
MGN: medial geniculate nuclei
MND: Motor neuron disease
MNI152: Montreal Neurological Institute 152 standard space
MR: magnetic resonance
MRS: magnetic resonance spectroscopy
MT: Magnetisation transfer
MV-re: reuniens/medial ventral nuclei
Myo: Myoinositol
NAA: N-acetylaspartate
PBA: pseudobulbar affect
Pc: paracentral nuclei
PCL: pathological crying and laughing
Pf: parafascicular nuclei
PLS: Primary lateral sclerosis
PMC: Primary motor cortex
Pt: paratenial nuclei
pTDP-43: phosphorylated 43 kDa TAR DNA-binding protein
PuA: pulvinar anterior nuclei
PuI: pulvinar inferior nucleus
PuL: pulvinar lateral nucleus
PuM: pulvinar medial nucleus
RE: Repeat expansion
SBMA: Spinal and bulbar muscular atrophy / Kennedy's disease
SD: standard deviation
SE: standard error
SOD1: superoxide dismutase 1
SPSS: statistical product and service solutions
T1: Timepoint 1
T1W: T1-weighted imaging
T2: Timepoint 2
TBSS: Tract-based spatial statistics
TE: Echo time
TFCE: threshold-free cluster enhancement
TI: Inversion time
TIV: Total Intracranial Volume
TR: repetition time
UMN: Upper motor neuron
VA: ventral anterior nuclei
VAmc: ventral anterior magnocellular nuclei
VBM: Voxel-based morphometry
VLa: ventral lateral anterior nuclei
VLp: ventral lateral posterior nuclei
VM: ventromedial nuclei
VPL: ventral posterolateral nuclei